

Microbial Iron Respiration Can Protect Steel from Corrosion

M. Dubiel,¹ C. H. Hsu,² C. C. Chien,¹ F. Mansfeld,² and D. K. Newman^{1*}

Division of Geological and Planetary Sciences, California Institute of Technology, Pasadena, California 91125,¹ and Corrosion and Environmental Effects Laboratory, Department of Materials Science and Engineering, University of Southern California, Los Angeles, California 90089-0241²

Received 11 September 2001/Accepted 12 December 2001

Microbiologically influenced corrosion (MC) of steel has been attributed to the activity of biofilms that include anaerobic microorganisms such as iron-respiring bacteria, yet the mechanisms by which these organisms influence corrosion have been unclear. To study this process, we generated mutants of the iron-respiring bacterium *Shewanella oneidensis* strain MR-1 that were defective in biofilm formation and/or iron reduction. Electrochemical impedance spectroscopy was used to determine changes in the corrosion rate and corrosion potential as a function of time for these mutants in comparison to the wild type. Counter to prevailing theories of MC, our results indicate that biofilms comprising iron-respiring bacteria may reduce rather than accelerate the corrosion rate of steel. Corrosion inhibition appears to be due to reduction of ferric ions to ferrous ions and increased consumption of oxygen, both of which are direct consequences of microbial respiration.

Microbes perform oxidation and reduction reactions that profoundly affect the stability of minerals in the environment, with consequences ranging from the promotion of acid mine drainage (19) to the bioremediation of organically polluted groundwater (7). In industrial settings, perhaps the most familiar metal transformation is the rusting of iron and steel, and microbes are thought to play an important role in this process (1). Microbiologically influenced corrosion (MC) can be a serious industrial problem and affects diverse processes ranging from water distribution in cast iron mains and sewers to transport of natural gas in steel pipelines. It has been estimated that for the United States oil industry alone, MC causes hundreds of millions of dollars in damage to the production, transport, and storage of oil every year (3). Yet the mechanistic basis of MC, despite its importance, has remained unclear.

A prevailing theory of MC holds that biofilms promote corrosion by inducing the formation of corrosion cells. This is thought to occur as a consequence of aerobic respiratory activity within biofilms that leads to the establishment of local cathodic and anodic regions on the steel surface, which promotes electron flow (6). Recent evidence, however, suggests that aerobically respiring bacteria may protect steel from corrosion over the long term (5), which raises questions regarding the extent to which aerobic respiration contributes to MC. Other explanations for MC include corrosion promotion by anaerobes such as sulfate-reducing and iron-reducing bacteria. Current theories maintain that sulfate reducers promote corrosion by consuming hydrogen and inducing ferrous sulfide formation and that iron reducers promote corrosion by reductively dissolving the protective ferric oxide coating that forms on the steel surface (6, 17). Biofilm communities that develop on the surfaces of corroding materials in natural environments are heterogeneous, and therefore there is significant uncer-

tainty concerning how these communities affect corrosion in any given environment.

Our goal was to take a reductionist approach to study the complex problem of MC. Specifically, we sought to create a single-species biofilm system to determine under what conditions and by which mechanisms actively respiring bacteria influence the corrosion of steel. We selected *Shewanella oneidensis* strain MR-1 (13) as the model organism for this study because it is amenable to genetic manipulation and is closely related to bacteria that have been isolated from corroding steel pipelines (20). *S. oneidensis* is a member of the gamma subdivision of the *Proteobacteria* and is a facultative anaerobe that can respire by using oxygen or ferric iron as its terminal electron acceptor. Thus, the respiratory versatility of *S. oneidensis* provided an opportunity to generate specific mutants to test the competing hypotheses about the effects of aerobic respiration and iron respiration on MC and to determine which effect dominates in a biofilm system in which both processes could occur.

Two mutant strains were generated by transposon mutagenesis. Transposon insertions were made by mating *S. oneidensis* strain MR-1 with *Escherichia coli* strain B-2155 containing pBSL180, a suicide plasmid carrying a mini-Tn10 transposon derivative marked with a kanamycin cassette. Exconjugants were selected on LML medium (2) supplemented with 50 µg of kanamycin per ml under aerobic conditions. The mutants were inoculated into 96-well microtiter plates filled with Luria-Bertani medium containing kanamycin and allowed to grow overnight. Each microtiter plate was processed to identify mutants defective in biofilm formation (16). Iron reduction mutants were identified as previously described (15).

One representative biofilm mutant and one representative iron reduction mutant were selected for further study (Fig. 1A). The biofilm mutant contained an insertion in the *fljI* gene that encodes a protein necessary for the synthesis of flagella. The *S. oneidensis* FliI homolog exhibits 68% identity and 82% similarity to the FliI protein of *Vibrio parahaemolyticus*, as determined by a pairwise amino acid alignment performed with the National Center for Biotechnology Information pro-

* Corresponding author. Mailing address: Division of Geological and Planetary Sciences, California Institute of Technology, Pasadena, CA 91125. Phone: (626) 395-6790. Fax: (626) 683-0621. E-mail: dkn@gps.caltech.edu.

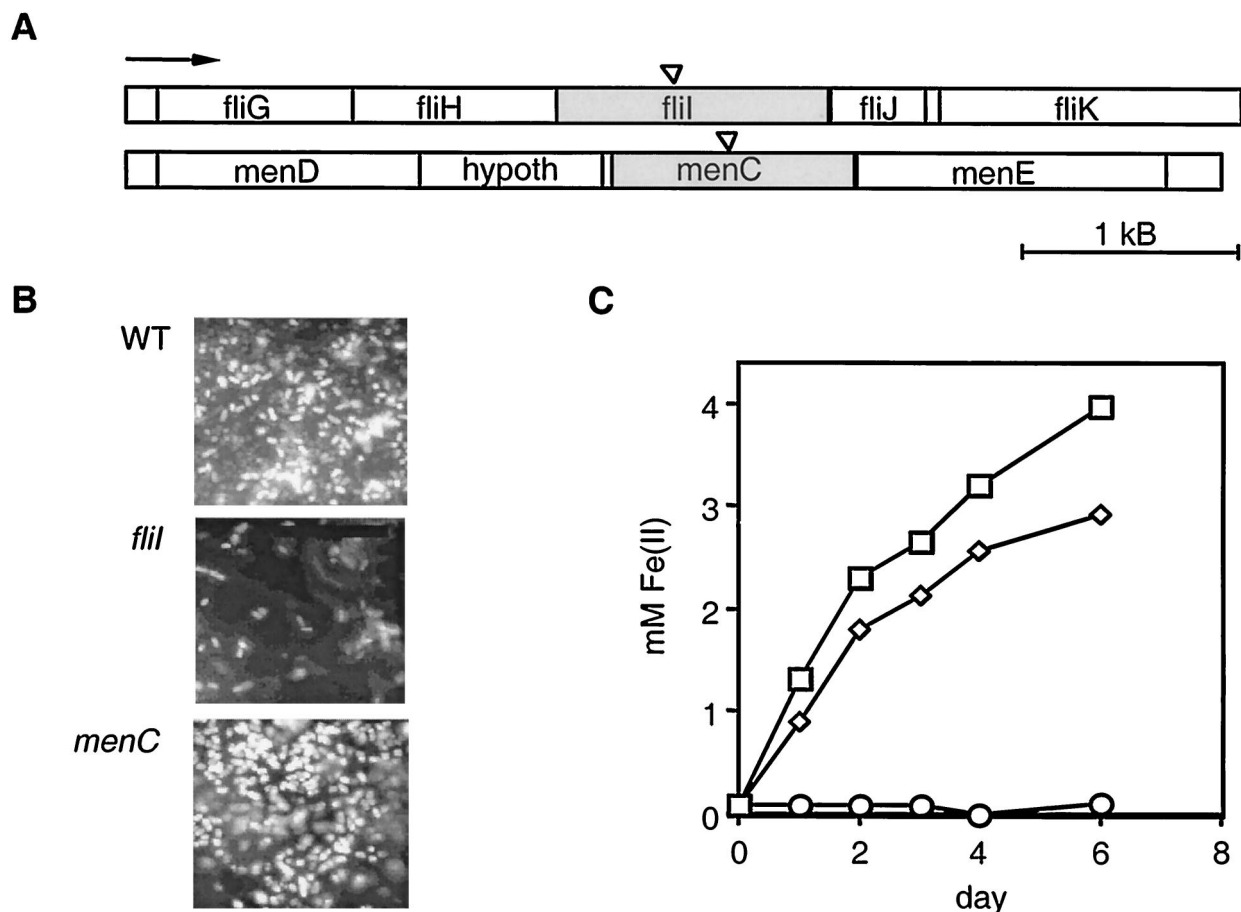


FIG. 1. Identities and phenotypes of the *S. oneidensis* mutants. (A) The biofilm mutant and the iron reduction mutant were generated by transposon insertion (indicated by triangles) into the *fliI* gene and the *menC* gene, respectively. These genes lie on different parts of the chromosome, and the flanking regions on either side of the disrupted genes are shown. The arrow indicates the direction of transcription for all open reading frames. The open reading frames are labeled on the basis of homology to known *E. coli* genes. *hypoth*, hypothetical gene. (B) Attachment of the *fliI* and *menC* mutants and the wild type (WT) to 1018 steel after 24 h. Light spots are DAPI-stained cells. Bar = 10 μm . (C) Reduction of goethite to Fe(II) over time for representative cultures. Symbols: \square , wild type; \diamond , *fliI* mutant; \circ , *menC* mutant.

gram BLAST2. Flagellar motility has been shown to be critical for the initial stages of biofilm formation in other gamma proteobacteria (18). The iron respiration mutant contained an insertion in the *menC* gene that encodes an enzyme necessary for the synthesis of menaquinone, a lipophilic electron carrier in the respiratory chain that conveys electrons to low-potential electron acceptors like iron; menaquinone is not necessary for electron transport to oxygen, and thus the *menC* mutant behaves normally with respect to aerobic respiration (11, 15).

Attachment assays were performed with 5-mm-diameter carbon steel chips (thickness, approximately 0.5 mm) obtained from Executiv Inc., Guatemala City, Guatemala. Sterilized chips were placed concave side up in a 96-well microtiter dish with 125 μl of LML medium. The wells were inoculated with 3 μl of the appropriate overnight culture and incubated for 24 h at 30°C. The chips were then rinsed in LML medium containing 5% formaldehyde to fix the cells, vigorously vortexed, and stained with 4',6'-diamidino-2-phenylindole (DAPI). Differences in bacterial cell attachment to the chips were determined by fluorescent light microscopy. As expected, the *fliI* mutant was nonmotile and was strongly defective in attachment to and

biofilm formation on the steel surfaces over time. The *menC* mutant, in contrast, attached as well as the wild type and formed normal biofilms (Fig. 1B).

The abilities of the mutants to reduce both soluble and solid forms of ferric iron [Fe(III)] were also determined. Anaerobic LML medium supplemented with 20 mM ferric citrate [for soluble Fe(III) reduction assays] or with 20 mM goethite [for solid Fe(III) reduction assays] was inoculated with the appropriate *Shewanella* strain by using standard anaerobic techniques (12). Reduction of Fe(III) to ferrous iron [Fe(II)] was measured by the ferrozine assay (21) with a Beckman DU 640 spectrophotometer at 564 nm. The wild type and the *fliI* mutant reduced soluble Fe(III) to Fe(II) at the same rate, whereas the *menC* mutant was completely blocked in this process. When grown on solid Fe(III) (e.g., α -FeOOH, synthetic goethite), however, the *fliI* mutant reduced iron at a lower rate than the wild type (Fig. 1C), presumably because direct contact between cells and minerals facilitates (but is not essential for) electron transfer in this organism (14).

Having genetically separated biofilm formation from iron reduction, we were able to determine the effects of microbial

attachment and respiration on corrosion. Electrochemical impedance spectroscopy (EIS) was used to determine how the mutants influenced the corrosion potential (E_{corr}) and corrosion rate of 1018 steel compared to the effects of the wild type and an uninoculated control. Because EIS is a nondestructive technique, it allows the corrosion rate for a given material to be monitored in a test cell whose solution chemistry can be manipulated and measured over time. Mild steel 1018 coupons (3 by 3 in.; Metal Samples, Inc.) were sterilized, weighed, and placed in the base of a glass corrosion chamber with an exposed area of 20 cm². Then 75 ml of LML medium was added to the chamber. An autoclavable Ag/AgCl electrode was used as the reference electrode, and stainless steel 316 was used as the counterelectrode. Impedance spectra were recorded with an applied alternating current signal of 20 mV (rms) and a frequency range from 10⁵ to 10 × 10⁻³ Hz by using Gamry equipment. The EIS data were analyzed by using the BASICS module of the ANALEIS software (10).

For each experiment, we recorded the changes in the impedance spectrum determined at the E_{corr} , the concentrations of Fe(III) and Fe(II) in solution, and the planktonic cell numbers daily. The initial impedance measurements were taken after 4 h, and then 1 ml of a fresh overnight culture was added to the chamber. The chamber was heated to 30°C, and the temperature was kept constant for the rest of the experiment. Impedance spectra were recorded every 24 h for five additional days. At the end of the experiment, the steel coupons were rinsed in water, DAPI stained, and observed with a fluorescent light microscope to assess biofilm formation. Biofilm formation on the steel coupons followed the pattern of attachment observed with the steel chips (e.g., the wild type and *menC* mutant formed normal biofilms, whereas the *fliI* mutant was less dense). Nevertheless, coverage was not uniform over the surfaces of the coupons for any strain. Such patchiness appears to be the rule for the majority of biofilms that have been examined (4). Subsequently, the chips were washed in 0.5 M HCl containing 3.5 g of hexamethylene tetramine per ml for 10 min and weighed to determine differences in mass loss. The EIS data were displayed as Bode plots in which the logarithm of the impedance modulus ($|Z|$) was plotted versus the logarithm of the frequency (f) of the applied alternating current signal. When the frequency of an applied signal is low ($f \rightarrow 0$), the impedance measurements reflect the polarization resistance (R_p), which is inversely proportional to the corrosion rate (8).

Figure 2 shows representative Bode plots obtained for 1018 steel in parallel experiments for chambers containing the wild type, the *fliI* mutant, the *menC* mutant, and an uninoculated control. Initial impedance spectra were recorded 4 h after inoculation with bacteria and were the same for all test cells. After 5 days of static incubation, significant differences in the low-frequency part of the impedance spectra were observed. The general shape of the impedance spectra, which in this case corresponds to a parallel combination of the electrode capacitance and R_p (9), did not differ in the presence of the different strains. This indicates that although the corrosion rates changed, the corrosion mechanism remained the same. Compared to the uninoculated control, the wild type and the *fliI* mutant maintained R_p at a high level (although the R_p maintained by the *fliI* mutant was lower than the R_p maintained by the wild type). The *menC* mutant maintained R_p at a lower

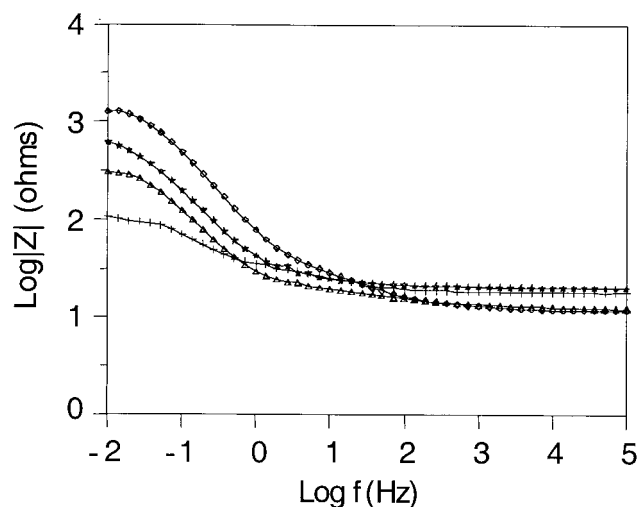


FIG. 2. Representative Bode plots obtained after 5 days of static incubation for the wild type, the *fliI* and *menC* mutants, and an uninoculated control. The curves represent independent EIS runs for parallel cultures. Symbols: \diamond , wild type; \star , *fliI* mutant; \triangle , *menC* mutant; $+$, uninoculated control. The logarithm of the impedance modulus ($|Z|$) is plotted versus the logarithm of the frequency (f) of the applied alternating current signal. When the frequency of the applied signal was very low ($f \rightarrow 0$, left side of the spectrum), impedance recordings reflected the R_p at the surface of the test electrode (in this case, 1018 steel). When the frequency was very high (right side of the spectrum), impedance recordings reflected the electrolyte resistance in solution. R_p is inversely proportional to the corrosion rate.

level than both the wild type and the *fliI* mutant but still provided better corrosion protection than the uninoculated control. The planktonic cell concentrations were approximately the same for all cultures, on the order of 10⁷ cells/ml. In these experiments, mass loss from the steel coupons was greatest for the uninoculated control (corresponding to a corrosion rate of 0.4 mg · cm⁻² · day⁻¹), a factor of 2 less for the *menC* and *fliI* mutants, and a factor of 4 less for the wild type.

From impedance data acquired at the E_{corr} to construct Bode plots, the relative corrosion rate ($\log [1/R_p]$) can be determined (9). Figure 3 shows a comparison of the changes in E_{corr} , relative corrosion rate, and concentration of ferrous ions in solution induced by the wild type over a 5-day period to the changes induced by the *fliI* and *menC* mutants and an aerobic uninoculated control. In a neutral, aerated solution, E_{corr} is the potential at which the rate of the metal dissolution reaction equals the rate of the oxygen reduction reaction. Prior to inoculation, the E_{corr} values for all corrosion cells were very similar, but by the end of the experiment, the E_{corr} values for both the uninoculated control and the *menC* mutant had decreased, whereas the E_{corr} values for the *fliI* mutant and the wild type had increased significantly (Fig. 3A). The increase in E_{corr} values was slower for the *fliI* mutant than for the wild type. In contrast, the corrosion rate remained high for the uninoculated control yet decreased over time for all strains; the lowest corrosion rates were observed for the wild type, followed by the *fliI* mutant and the *menC* mutant (Fig. 3B).

These trends are related to the amount of Fe(II) measured in solution over time; the highest Fe(II) concentrations were observed for the wild type, moderate values were obtained for

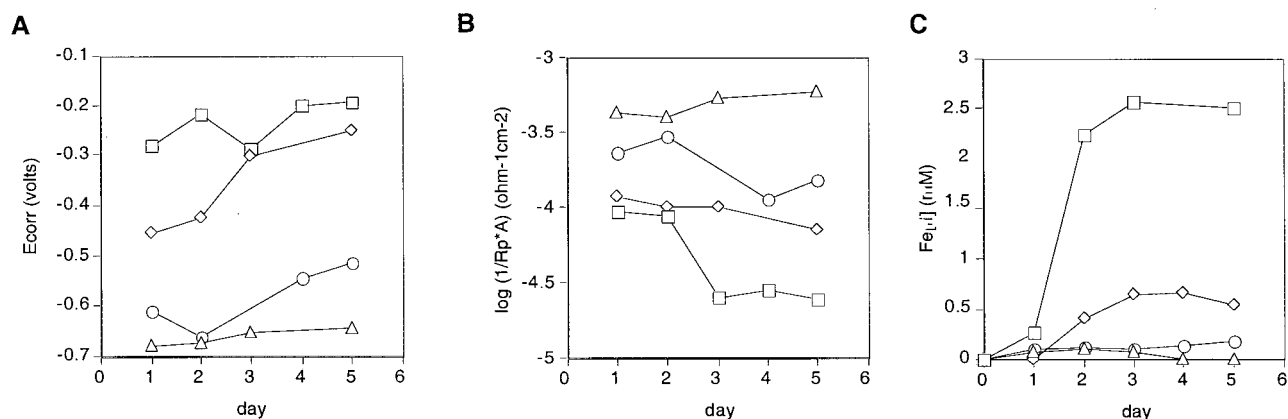


FIG. 3. E_{corr} (A), relative corrosion rate per unit area (A) ($1/R_p \cdot A$, expressed in ohm $^{-1}$ ·centimeter $^{-2}$) (B), and ferrous iron concentration (C) in solution as a function of exposure time. The data are from a 5-day static incubation experiment in which we compared the behavior of the wild type (□) to the behavior of the *flil* mutant (◇), the *menC* mutant (○), and an uninoculated control (△). The data are representative of the data obtained in five independent experiments for each strain or control.

the *flil* mutant, and low values were obtained for the *menC* mutant and the uninoculated control (Fig. 3C). The small amounts of Fe(II) measured in solution for the *menC* mutant and the uninoculated control reflect the balance between the Fe(II) formed by oxidation of the metallic iron Fe(0) in 1018 steel and the Fe(II) remaining in solution prior to its oxidation to Fe(III) by reaction with dissolved oxygen. This was visually evident; the chamber containing the wild type remained completely clear throughout the experiments (with the exception of a small amount of oxidized iron that appeared at the air-liquid interface), the chamber containing the *flil* mutant also was relatively clear (although not as clear as the chamber containing the wild type), and the chamber containing the *menC* mutant had a rusty color throughout. In the uninoculated chamber a thick porous layer of goethite accumulated on the steel surface over time under aerobic conditions, but the chamber remained clear under anaerobic conditions. These visual differences mirrored the relative abilities of the wild type and the mutants to perform anaerobic respiration using solid iron (Fig. 1C). In general, the higher the Fe(II) concentration, the higher the E_{corr} maintained in the system and the lower the corrosion rate.

These results suggested that the concentration of Fe(II) in solution was a critical variable in corrosion inhibition. To test this hypothesis, we performed week-long EIS experiments with *Vibrio cholerae* strain El Tor N16961 [another gamma proteobacterium that is similar to *S. oneidensis* but cannot respire Fe(III)] and a different iron reduction mutant of *S. oneidensis* identified in our screening analysis (this mutant contained a transposon insertion in a gene that was 100% identical, as determined by a pairwise alignment using BLAST, to the *S. oneidensis* strain MR-1 *mtrB* gene [2]). These experiments were performed by using the procedures described above for the experiments performed with the wild-type, *flil*, and *menC* strains. As predicted, the E_{corr} , corrosion rate, and concentration of Fe(II) in the medium for these strains were about the same as those measured for the *menC* mutant (data not shown). Because all of the strains could form normal biofilms and still decreased corrosion—albeit not as effectively as strains

that could also respire Fe(III)—these data argue against the notion that biofilm-induced corrosion cells promote corrosion.

Further support for the hypothesis that Fe(II) has a protective role came from a dilution-killing experiment performed with the wild type. In this experiment we compared the changes in the E_{corr} , the corrosion rate, and the concentration of ferrous iron in solution generated by the wild type over a 2-week period, subject to manipulation of the medium. As in the experiment described above, the E_{corr} remained high after 5 days of static incubation compared to the value obtained with the uninoculated control, yet once fresh medium was pumped into the chamber (day 5), the E_{corr} decreased to more negative values and decreased even further once the cells were killed by the addition of kanamycin (50 $\mu\text{g/ml}$) (day 9). As predicted, the corrosion rate remained low in the presence of active Fe(III)-respiring bacteria [even after dilution, as some Fe(II) remained in the system] but rose significantly after the addition of kanamycin. Although the concentration of planktonic cells remained the same (roughly 10^7 cells/ml) until the time of killing, the Fe(II) concentration rose and fell parallel to the changes in the E_{corr} . The pH remained circumneutral throughout the experiment.

We can interpret our data by using a theoretical representation of anodic and cathodic polarization curves. In Fig. 4A the potential is plotted versus the logarithm of the current density. Current density is proportional to the reaction rate. It is assumed that the anodic iron oxidation reaction is a charge transfer-controlled reaction resulting in a straight line, while for the cathodic oxygen reduction reaction it is assumed that the charge transfer-controlled reaction at a low current density is followed by the limiting current density for oxygen reduction (i_L) that depends on the oxygen concentration in the bulk solution. The corrosion reaction for iron in aerated, neutral media is diffusion controlled; i.e., the corrosion current density (i_{corr}) equals the limiting current density (i_L). Since aerobic respiration consumes oxygen, i_L decreases, resulting in a decrease in E_{corr} (as observed for the *menC* mutant, which forms a normal biofilm and respire aerobically). Fe(III) respiration by bacteria increases the concentration of Fe(II) in solution,

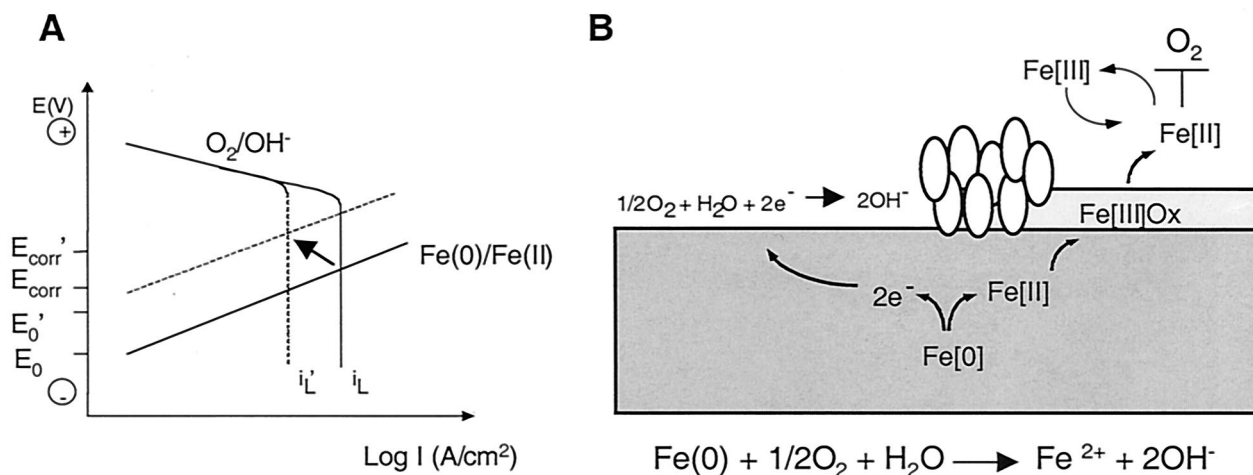


FIG. 4. Model for corrosion protection based on microbial respiration of oxygen and iron. (A) Theoretical polarization curves for corrosion of iron in a neutral, aerated solution. The straight lines correspond to the iron oxidation reaction that is under charge transfer control. The polarization curves for oxygen reduction consist of a charge transfer-controlled reaction at low current densities, followed by a limiting current density (i_L) for the reduction of oxygen, which is under mass transport control. The E_{corr} and the corrosion current density (i_{corr}) are located at the intersection of the polarization curves for the oxidation and reduction reactions. The arrow indicates the direction of the expected shift in the curves in a system with wild-type *S. oneidensis*. (B) Diagram showing how oxygen consumption that is mediated by direct microbial oxygen respiration and indirect reduction by ferrous iron (produced by ferric iron respiration) protects steel from corrosion. The general equation for corrosion is given. The ovals represent cells that are actively respiring at the steel surface. Ferrous iron produced by respiration of Fe(III) oxides forms a reducing shield that blocks oxygen from attacking the steel surface.

shifting the reversible potential for the Fe(0)/Fe(II) couple to more positive values (E'_{O}) than those under the initial conditions (E_{O}).

The observed decrease in i_{corr} and increase in E_{corr} (for the wild type and the *fliI* mutant) can only be explained by a simultaneous increase in E_{O} and decrease in i_L , resulting from an increase in the Fe(II) concentration and oxidation of Fe(II) by oxygen to Fe(III). The Fe(III) formed is then reduced by the bacteria to Fe(II), which forms a protective shield against oxygen attack on the steel surface (Fig. 4B). For the wild type (which forms biofilms and respire both aerobically and anaerobically) the positive shift for E_{corr} and the negative shift for i_{corr} are more striking than the shifts for the *fliI* mutant (which reduces iron more slowly and is less able to protect the steel surface due to its defect in biofilm formation). Due to the inherent patchiness of the biofilms on the steel coupons (as exemplified by the wild-type and *menC* strains), oxygen respiration by bacteria cannot provide a complete barrier to oxygen attack at the steel surface. In contrast, diffusion of Fe(II) throughout the chamber provides a uniform chemical barrier and explains why corrosion protection was greatest with the strains that could reduce Fe(III).

Independent experiments to evaluate the effects of wild-type *S. oneidensis* strain MR-1 on the corrosion of mild steel, brass, and aluminum alloy 2024 (13a) confirmed that iron reduction plays a central role in this model of corrosion protection. In these experiments E_{corr} increased and i_{corr} decreased, results that are similar to the results obtained in the present study with mild steel, yet when *S. oneidensis* was placed in contact with brass or aluminum, E_{corr} and i_{corr} both decreased due to aerobic respiration. The shift of the anodic polarization curve for the Fe(0)-Fe(II) reaction (and hence an increase in E_{corr}) did not occur in these cases as biologically catalyzed

redox chemistry could not occur with these materials. Furthermore, in the case of 1018 steel, when the growth medium was changed to include phosphate, $\text{Fe}_3(\text{PO}_4)_2 \cdot 8\text{H}_2\text{O}$ (vivianite) formed instead of goethite, and no difference in corrosion protection was observed between the *menC* mutant and the wild type (Dubiel and Newman, unpublished data). This was expected because the ferrous iron in vivianite cannot be used as a terminal electron acceptor by *S. oneidensis*.

In conclusion, our results suggest that both aerobic respiration and anaerobic respiration can significantly contribute to corrosion protection in systems in which water is quiescent. Depending on the chemistry of the water in which Fe(0) oxidation occurs, in the presence of iron-reducing bacteria the resulting corrosion product(s) may play a protective role beyond merely preventing attack by oxygen by forming a physical barrier at the surface. If the corrosion product contains Fe(III), iron reducers may utilize this substrate as a terminal electron acceptor for anaerobic respiration, and the resulting Fe(II) may scavenge oxygen in the water column. Although biofilms in environments in which corrosion is a problem are not limited to single species, such as *S. oneidensis*, our results point to a general principle: biofilms may be beneficial in the context of corrosion. Indeed, the physiology of the bacteria that comprise a biofilm and the flow rate and chemistry of the water which they inhabit to a large extent determine the ultimate impact of the microorganisms on corrosion.

We thank G. Rossman and E. Arredondo for help with mineral identification, P. Watnick for providing *V. cholerae* strain El Tor N16961, and J. Huang and R. Kolter for contributions to earlier versions of this work. Preliminary sequence data were obtained from The Institute for Genomic Research website at <http://www.tigr.org>. Sequencing of *S. oneidensis* was accomplished with support from the Department of Energy.

Support was provided by a grant from the Office of Naval Research to D.K.N.

REFERENCES

1. **Angell, P.** 1999. Understanding microbially influenced corrosion as biofilm-mediated changes in surface chemistry. *Curr. Opin. Biotechnol.* **10**:269–272.
2. **Beliaev, A. S., and D. A. Saffarini.** 1998. *Shewanella putrefaciens mtrB* encodes an outer membrane protein required for Fe(III) and Mn(IV) reduction. *J. Bacteriol.* **180**:6292–6297.
3. **Costerton, J. W., and J. Boivin.** 1987. Microbially influenced corrosion, p. 56–76. *In* M. W. Mittelman and G. G. Geesey (ed.), *Biological fouling of industrial water systems. A problem solving approach.* Water Micro Associates, San Diego, Calif.
4. **Costerton, J. W., and P. S. Stewart.** 2001. Battling biofilms. *Sci. Am.* **285**: 74–81.
5. **Jayaraman, A., J. C. Earthman, and T. K. Wood.** 1997. Corrosion inhibition by aerobic biofilms on SAE 1018 steel. *Appl. Microbiol. Biotechnol.* **47**:62–68.
6. **Little, B. J., P. A. Wagner, and Z. Lewandowski.** 1997. Spatial relationships between bacteria and mineral surfaces, p. 123–159. *In* J. F. Banfield and K. H. Nealson (ed.), *Geomicrobiology: interactions between microbes and minerals.* Mineralogical Society of America, Washington, D.C.
7. **Lovley, D. R., C. J. Woodward, and F. H. Chapelle.** 1994. Stimulated anoxic biodegradation of aromatic hydrocarbons using Fe(III) ligands. *Nature* **370**: 128–131.
8. **Mansfeld, F.** 1976. The polarization resistance technique for measuring corrosion currents, p. 163–262. *In* M. G. Fontana and R. W. Staehle (ed.), *Advances in corrosion science and technology*, vol. 6. Plenum Press, New York, N.Y.
9. **Mansfeld, F., and W. J. Lorenz.** 1991. Electrochemical impedance spectroscopy (EIS): application in corrosion science and technology, p. 581–647. *In* R. Varma and J. R. Selman (ed.), *Techniques for characterization of electrodes and electrochemical processes.* Wiley, New York, N.Y.
10. **Mansfeld, F., H. Shih, H. Greene, and C. H. Tsai.** 1993. Analysis of EIS data for common corrosion processes. ASTM (Am. Soc. Test Mater.) Spec. Tech. Publ. **1188**:37.
11. **Meganathan, R.** 1996. Biosynthesis of menaquinone and ubiquinone, p. 642–656. *In* F. C. Neidhardt et al., (ed.), *Escherichia coli and Salmonella typhimurium: cellular and molecular biology*, vol. 1. American Society for Microbiology, Washington, D.C.
12. **Miller, T. L., and M. J. Wolin.** 1974. A serum bottle modification of the Hungate technique for cultivating obligate anaerobes. *Appl. Microbiol.* **27**: 985–987.
13. **Myers, C., and K. H. Nealson.** 1988. Bacterial manganese reduction and growth with manganese oxide as the sole electron acceptor. *Science* **240**: 1319–1320.
- 13a. **Nagiub, A., and F. Mansfeld.** Evaluation of microbiologically influenced corrosion inhibition (MICI) with EIS and ENA. *Electrochim. Acta*, in press.
14. **Newman, D. K.** 2001. How bacteria respire minerals. *Science* **292**:1312–1313.
15. **Newman, D. K., and R. Kolter.** 2000. A role for excreted quinones in extracellular electron transfer. *Nature* **405**:94–97.
16. **O'Toole, G. A., L. A. Pratt, P. I. Watnick, D. K. Newman, V. B. Weaver, and R. Kolter.** 1999. Genetic approaches to the study of biofilms. *Methods Enzymol.* **310**:91–109.
17. **Potekhina, J. S., N. G. Sherisheva, L. P. Poverkina, A. P. Pospelov, T. A. Ralotoma, F. Warnecke, and G. Gottschalk.** 1999. Role of microorganisms in corrosion inhibition of metals in aquatic systems. *Appl. Microbiol. Biotechnol.* **52**:639–646.
18. **Pratt, L. A., and R. Kolter.** 1999. Genetic analyses of bacterial biofilm formation. *Curr. Opin. Microbiol.* **2**:598–603.
19. **Schrenk, M. O., K. J. Edwards, R. M. Goodman, R. J. Hamers, and J. F. Banfield.** 1998. Distribution of *Thiobacillus ferrooxidans* and *Leptospirillum ferrooxidans*: implications for generation of acid mine drainage. *Science* **279**: 1519–1522.
20. **Semple, K. M., and D. W. S. Westlake.** 1987. Characterization of iron-reducing *Alteromonas putrefaciens* strains from oil field fluids. *Can. J. Microbiol.* **33**:366–371.
21. **Stookey, L. L.** 1970. Ferrozine: a new spectrophotometric reagent for iron. *Anal. Chem.* **42**:779–781.